CORRECTION OF THERMOGRAPHIC MEASUREMENTS IN THE PRESENCE OF PARTICIPATING GASES

Gilberto Maurer, gilberto.maurer@yahoo.com.br
Marcelo M. Galarça, mgalarca@mecanica.ufrgs.br
Francis H. R. França, frfranca@mecanica.ufrgs.br
Departamento de Engenharia Mecânica – Universidade Federal do Rio Grande do Sul – UFRGS – Porto Alegre, RS, Brazil

Abstract. *This work presents a methodology to correct the measurement of temperature by thermograph in the presence of participating media. In the measurement of the temperature of a surface, the incident thermal radiation on the thermograph sensor can be affected by emission and absorption of the participating medium between the surface and the sensor. For the correction of the measurement, it is necessary to consider the composition and temperature of the medium, and the path length the radiation intensity travels in the medium. The methodology is based on the solution of the radiative transfer equation along the path length, considering absorption and emission of the medium, but not scattering. The methodology is applied to a gaseous mixture that is typically formed in the combustion of methane in air, with a molar concentration of 20% of water vapor, 10% of carbon dioxide, and 80% of inert gas. The radiative properties of the medium are treated by the weighted-sum-of-gray-gases model, using relations that have been recently available. Due to the practical applications of the proposed methodology, correlations were developed for the correction of the temperature indicated by thermograph.*

Keywords: Thermography, temperature measurement, participating media, combustion gases, WSGG model

1. INTRODUCTION

Thermography is an important technique for remote temperature measurements, with an important application in systems where the measurement by direct contact between the sensor and the surface is not possible. Typical examples include internal surfaces of gas turbines, furnaces and other combustion systems, which must be constantly monitored to prevent overheating and failure. The physical mechanism behind the measurement is the thermal radiation that is emitted from the surfaces. However, for an accurate measurement, there are some difficulties that must be overcome, such as the lack of information concerning the total hemispherical emissivity of the surface, and how much of the energy that leaves the surface is emission and reflection. In several cases, the surfaces can be assumed ideally black, so these two aspects are readily solved: the emissivity is equal to the unity and no radiation leaves the surface due to reflection. For instance, in combustion chambers, the surfaces are covered with soot, so the assumption of blackbody is a close approximation to reality (Siegel and Howell, 2002).

Another difficulty arises when the measurement is made in the presence of participating gases, such as water vapor and carbon dioxide, since the thermal radiation measured in the thermograph is affected by the emission and absorption of the gases. The neglect of the absorption and the emission of the gases can lead to considerable errors, overestimating or underestimating the temperature of the surface when the gases have a higher or lower temperature, respectively. Gas radiation presents a complex dependence of the composition, temperature and optical thickness, which should be accounted in the measurement. Radiation in participating media has been extensively studied because of its importance in several applications in engineering. Often the thermal radiation is the main heat transfer mechanism when there are combustion gases at high temperature.

The most accurate way to determine the radiative heat transfer is, possibly, the line-by-line (LBL) integration of the radiative transfer equation (Dennison and Webb, 1995). This integration involves the calculation of hundreds of thousands of lines arranged in the absorption spectrum, which requires a great computational effort. In practical situations, which require the calculation of radiative heat transfer in participating gases, spectral gas models are used. The simplest of these models is the gray gas model, in which the absorption coefficient is independent of wavelength. This model shows large deviations from the expected behavior of real gases, but it is still often used. The weighted-sum-of-gray-gases (WSGG), proposed by Hottel and Sarofim (1967), models the entire spectrum considering a few bands with uniform absorption coefficients, where each band is interpreted as a gray gas. Taylor and Forester (1974) also obtained similar correlations from fitting semi-empirical data. Smith et al. (1982) obtained weighting functions and absorption coefficients of gray gases for fitting data generated from the exponential wide-band model. Galarça et al. (2008) presented new correlations for the weighted-sum-of gray-gases model and absorption coefficients to use in an efficient computational model. These correlations were built from data of total emissivities obtained by the Monte Carlo method applied to the absorption-line blackbody distribution function (ALBDF), described in Maurente et al. (2007), which considers in detail the expected behavior of the participant media. It is expected that these correlations are more accurate than those proposed by Smith et al. (1982).

The correlations of Galarça et al. (2008) are valid for gaseous mixtures that are generated in stoichiometric combustion of two typical fuels, methane and fuel oil. The products of the methane combustion contain 20% of water

vapor, 10% of carbon dioxide and 70 % of inert gas (air or nitrogen, for instance). The results were obtained for a total pressure of 1.0 atm, gas temperatures ranging from 400 K to 2400 K, and pressure-path length products from 0.001 to 10 atm·m. A Levenberg-Marquardt non-linear regression method was used to fit the data and supply the absorption coefficients and the temperature dependent weights.

This work presents a methodology to make the correction of thermographic measurements in the presence of combustion gases from the stoichiometric combustion of methane. The correction is based on the solution of the radiative transfer equation, which is solved in the direction of the measurement path. The radiative properties of the gaseous mixture are modeled with the correlations provided by Galarça et al. (2008). Practical correlations for direct application are presented based on numerical solutions, relating the actual temperature of the surface to the temperature indicated in the sensor, the temperature of the gases, and the distance between the surface and the sensor.

3. PROBLEM ANALYSIS

3.1. Thermograph Cameras

The equipment for thermographic measurement is also known as infrared camera; it operates similarly to a conventional camcorder, but can capture images in a different range of wavelength. In general, the thermograph cameras used in industry captures images in the infrared range of 8 to 14 μm. The cameras can operate in total darkness because the level of ambient light does not interfere in the measurement. The images are formed from the radiation measurement of the surface. Each pixel of the image corresponds to a point that is measured, and is equivalent to many pyrometers directed to the same region. The resolution of these cameras is considerably smaller than the optical cameras, most thermographs produces images with 160×120 or 320×240 pixels. These images may be color or black and white and the colors represent the temperature of the surface. Therefore, a scale should be positioned next to the image, comparing the colors with the corresponding temperatures.

According to Holman (1994), the temperature of a surface can be determined from the following relation:

$$T = \left(\frac{E}{\varepsilon \sigma} \right)^{1/4} \tag{1}$$

where T is the estimated temperature, E is the emissive power that is measured in the sensor, ε is the surface emissivity, and σ is the Stefan-Boltzmann constant (σ = 5,670 E-08 W/m^2·K^4). In equation (1), a few assumptions are implicit: 1) the reflection from the surface is negligible in comparison to emission; 2) the surface emissivity is known; and 3) between the surface and sensor the medium is non-participating or transparent.

The thermograph cameras can be classified into two categories: with common sensors or chilled. The cameras with chilled sensors have higher sensitivity, because the temperature of the sensor (between 4 and 110K) remains considerably below the temperature of the surface that is to be measured. In general, these thermographs require a closed chamber vacuum. The cooling of the sensors allows a better response, without the interference of radiation of the measuring equipment. However, the use of this type of camera is restricted by the high cost of specific materials for use in low temperatures and pressures, in addition to the time that is required to reach the desired temperature of the sensors and to the large space it occupies.

The cameras with normal sensors, which operate at ambient temperature, are the most used due to ease of portability, handling, and also because they have the most affordable price. The modern thermographs use sensors that work with the change of resistance, voltage or current caused by the infrared radiation received. This variation is measured and compared with the sensor operation temperature. Images are made which may be further processed to facilitate the understanding of the measurement of the surface temperature field.

3.2 Physical Analysis

In this problem, the measured surface is assumed to be black. In several engineering systems, surfaces are oxidized or covered with impurities or soot, so the assumption of blackbody can be a close approximation to reality. It follows that the emissivity of the surface can be set as the unit ($\varepsilon = 1$). Since black surfaces are diffuse, it is also valid the equality $E_b = \pi I_b$, which relates the emissive power with the total intensity of radiation.

The radiation intensity that is emitted by the surface changes due to the absorption and emission of a participating medium. These changes depend on the distance between the sensor and the surface, the concentrations of the participating species and the average temperature, according to Fig. 1. For a medium composed of gases such as water vapor and carbon dioxide, scattering can be neglect, so the direction of the radiation intensity, contrarily to its magnitude, is not affected. The distance S is the length of participating media between the surface and the sensor.

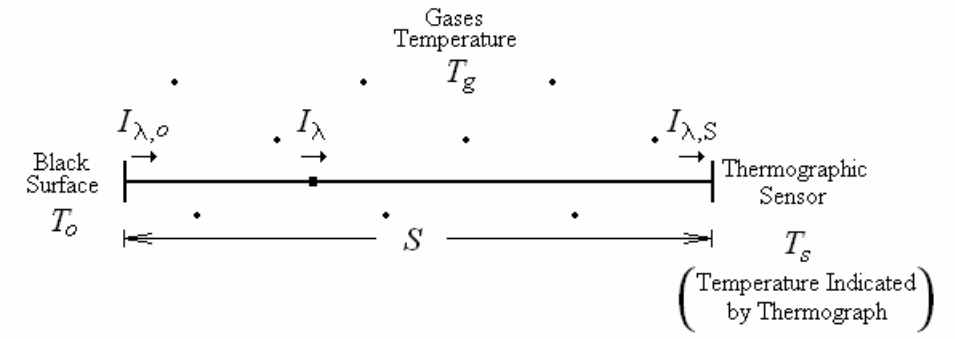

Figure 1. General outline of the problem.

The variation of the radiation intensity along the path *S* is given by the radiative transfer equation:

$$\frac{dI_\lambda}{ds} = a_\lambda I_{\lambda,b} - a_\lambda I_\lambda \tag{2}$$

where a_λ is the spectral absorption coefficient, and $I_{\lambda,b}$ is the spectral intensity of the blackbody at the temperature of the medium, T_g. In the right-hand side of equation (1), the first term accounts for emission in the medium, while the second term takes into account the absorption. Integrating equation (2) over the distance leads to:

$$\int_{I_{\lambda,0}}^{I_{\lambda,S}} \frac{dI_\lambda}{a_\lambda I_{\lambda,b} - a_\lambda I_\lambda} = \int_0^S dS \tag{3}$$

It follows that:

$$I_{\lambda,S} = I_{\lambda,b}\left[1 - \exp\left(-a_\lambda S\right)\right] + I_{\lambda,0}\exp\left(-a_\lambda S\right) \tag{4}$$

Equation (4) can be rewritten as:

$$I_{\lambda,S} = \varepsilon_\lambda I_{\lambda,b} + \tau_\lambda I_{\lambda,0} \tag{5}$$

where $\varepsilon_\lambda = 1 - \exp\left(-a_\lambda S\right)$ is the spectral emittance of the medium; and $\tau_\lambda = \exp\left(-a_\lambda S\right)$ is the spectral transmittance.

The total radiation intensity in the position *S* is given by the integration of the spectral intensity over the spectrum:

$$I_S = \int_\lambda I_{\lambda,S} d\lambda \tag{6}$$

Applying the weighted-sum-of-gray-gases (WSGG) model for the integration over the spectrum leads to:

$$I_S = \int_\lambda \left[1 - \exp\left(-a_\lambda S\right)\right] I_{\lambda,b} d\lambda + \int_\lambda \exp\left(-a_\lambda S\right) I_{\lambda,0} d\lambda \tag{7}$$

According to the WSGG model, the spectrum can be represented by bands with uniform absorption coefficients. Each band corresponds to a gray gas presented in the medium (Hottel and Sarofim, 1967). According to Smith *et al.* (1982) three bands are sufficient for a good approximation, as represented in Fig 2.

Therefore, the integral becomes a sum that takes into account the participating bands and transparent windows *TW* (intervals of wavelength where the absorption coefficient is null).

$$I_S = \sum_{l=1}^{L}\left\{\left[1 - \exp\left(-a_l S\right)\right]\int_{\Delta\lambda_l} I_{\lambda,b} d\lambda\right\} + \sum_{l=1}^{L}\left\{\exp\left(-a_l S\right)\int_{\Delta\lambda_l} I_{\lambda,0} d\lambda\right\} + \int_{TW} I_{\lambda,0} d\lambda \tag{8}$$

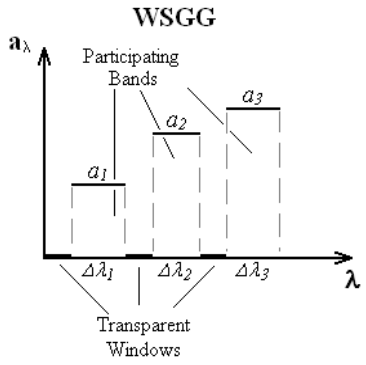

Figure 2. WSGG representation of the absorption coefficient in the spectrum.

The integrals $\int_{\Delta\lambda_l} I_{\lambda,b}d\lambda$ and $\int_{\Delta\lambda_l} I_{\lambda,0}d\lambda$ can be calculated from the blackbody fraction of total emission:

$$I_S = \sum_{l=1}^{L}\left\{\left[1-\exp(-a_l S)\right]F_{\Delta\lambda_l,Tg}I_{b,g}\right\}+\sum_{l=1}^{L}\left\{\exp(-a_l S)F_{\Delta\lambda_l,T0}I_{b,0}\right\}+\int_{TW} I_{\lambda,0}d\lambda \tag{9}$$

where:

$$C_l(T_g) = F_{\Delta\lambda_l,Tg} = \frac{\int_{\Delta\lambda_l} I_{\lambda,b}d\lambda}{\int_{\lambda} I_{\lambda,b}d\lambda} \tag{10}$$

$$\int_{\lambda} I_{\lambda,b}d\lambda = I_{b,g} = \frac{\sigma T_g^{\,4}}{\pi} \tag{11}$$

Equations (10) and (11) are applied in a similar manner for the temperature of the surface T_0.

Using $C_l(T_g)$ and $C_l(T_0)$ as correlating functions, the fraction of total emission is estimated as a function of temperature only. In this work, the correlations were obtained from Galarça *et al.* (2008).

For the transparent windows:

$$\left(\sum_{l=1}^{L}\int_{\Delta\lambda_l} I_{\lambda,0}d\lambda\right)+\int_{TW} I_{\lambda,0}d\lambda = \int_{\lambda} I_{\lambda,0}d\lambda = I_{b,0} \tag{12}$$

$$\frac{\sum_{l=1}^{L}\int_{\Delta\lambda_l} I_{\lambda,0}d\lambda}{I_{b,0}}+\frac{\int_{TW} I_{\lambda,0}d\lambda}{I_{b,0}} = 1 \tag{13}$$

$$\sum_{l=1}^{L} C_l(T_0)+\frac{\int_{TW} I_{\lambda,0}d\lambda}{I_{b,0}} = 1 \tag{14}$$

Therefore:

$$\int_{TW} I_{\lambda,0}d\lambda = \left[1-\sum_{l=1}^{L} C_l(T_0)\right]I_{b,0} \tag{15}$$

Combining equations (9), (10), (11) and (15) leads to the final relation of the radiation intensity measured in the sensor as a function of the surface intensity $I_{b,o}$, the gas intensity $I_{b,g}$, and the path length S:

$$I_S = \left\{\sum_{l=1}^{L}\left[1-\exp(-a_l S)\right]C_l(T_g)\right\}I_{b,g} + \left\{\sum_{l=1}^{L}\exp(-a_l S)C_l(T_0)\right\}I_{b,0} + \left[1-\sum_{l=1}^{L}C_l(T_0)\right]I_{b,0} \tag{16}$$

The blackbody radiation intensity can be related to the temperature by the following relations:

$$I_b = \frac{e_b}{\pi} = \frac{\sigma T^4}{\pi} \tag{17}$$

From the above relation, one obtains a final expression that depends solely on the temperature:

$$T_S^{\,4} = \left\{\sum_{l=1}^{L}\left[1-\exp(-a_l S)\right]C_l(T_g)\right\}T_g^{\,4} + \left\{\sum_{l=1}^{L}\exp(-a_l S)C_l(T_0)\right\}T_0^{\,4} + \left[1-\sum_{l=1}^{L}C_l(T_0)\right]T_0^{\,4} \tag{18}$$

The objective of the present analysis is to determine the temperature T_0. As seen in Fig. 1, T_0 is the temperature of the surface that is to be measured. Equation (18) shows that it depends on the temperature that is indicated in the thermograph (T_S), the average temperature of combustion gases (T_g), and the distance between the sensor and the surface (S). Implicitly, it also depends on the concentrations of the gaseous species through the WSGG coefficients and weighting functions.

3.2.1 The WSGG spectral absorption coefficients (a_l)

The WGSS model divides the spectrum into L regions, where the absorption coefficient is considered constant. This model is not restricted to the situation in which the band corresponding to a gas is continuous in a region. Unlike the situation that is shown in Fig. 2, each gray gas may occupy different positions in the spectrum.

For the stoichiometric combustion of methane (products of combustion: 20% of water vapor, 10% of carbon dioxide and air) there is a partial pressure (p) of 0.3 atm, corresponding to the participating gases. The spectral absorption coefficient is given by:

$$a_l = pk_l \tag{19}$$

The factors k_l for calculating the absorption coefficients are presented in Table 1.

Table 1. Factors for the absorption coefficients: 20% H_2O, 10% CO_2, 70% inert gas.
(Source: Galarça *et al.,* 2008)

Methane (p = 0.3 atm)	
l	k_l [1/(atm·m)]
1	0.517
2	9.559
3	161.988

3.2.2 The WSGG weighting functions ($C_l(T)$)

The weighted factors $C_l(T_0)$ and $C_l(T_g)$, used in the weighted-sum-of-gray-gases, are obtained from:

$$C_l(T) = \sum_{j=1}^{L} b_{i,j} T^{j-1} \tag{20}$$

where the coefficients $b_{i,j}$ are presented in Table 2.

Table 2. Coefficients for weighted factors 20% H_2O, 10% CO_2, 70% inert gas.
(Source: Galarça *et al.,* 2008)

Methane (p = 0.3 atm)				
l	$b_{i,1}x10^{1}$	$b_{i,2}x10^{4}$	$b_{i,3}x10^{7}$	$b_{i,4}x10^{11}$
1	2.801	3.244	-1.299	0.712
2	2.003	1.869	-1.394	5.454
3	1.240	-1.086	0.283	-0.114

3.2.3 Solution methodology

Equation (18) can be interpreted as an inverse problem, since it is given as an input value the temperature indicated in the thermograph (T_S), and the objective it to find the actual temperature of the surface (T_0). For the solution, it is necessary to develop an iterative process, because the unknown T_0 has to be determined, while it is necessary for the calculation of factors $C_l(T_0)$. The problem has a highly nonlinear behavior because the coefficients $C_l(T_0)$ present a has a fourth order dependence of T_0.

In the iterative process, the actual temperature of the surface, T_0, is first guessed, and then with equation (18) a new estimative of T_0 is made. This procedure is repeated until convergence achieved. In this paper, it is adopted as convergence an absolute difference of 10^{-4} K between the last two estimates of the temperature T_0. The algorithm was programmed using the Compaq Visual Fortran 6. Some results are discussed next, highlighting a few aspects of the methodology and of the problem itself.

4. RESULTS AND DISCUSSION

Using the proposed methodology, it is possible to correlate the values of the temperature indicated by the thermograph and the actual surface temperature. Typical results are presented in Fig. 3, which shows the actual temperature of the surface as a function of the temperature indicated in the thermograph, considering different distances *S*, and for a medium composed of 10% of water vapor and 10% of carbon dioxide at the temperature of 1400 K. As seen in the figure, when the medium temperature is at same value of the surface temperature, no deviation occurs between the actual temperature of the surface and the temperature indicated in the thermograph. When the temperatures are different, the largest is the path *S*, the largest is the deviation between the actual temperature of the sensor and the temperature indicated in the thermograph. For instance, considering the example in which the medium is at the temperature of 1400 K, and the actual temperature of the surface is T_0 = 1200 K, the temperatures indicated in the thermograph will be approximately 1320 K, 1340 K and 1355 K when the distances are 1 m, 5m and 10 m, respectively.

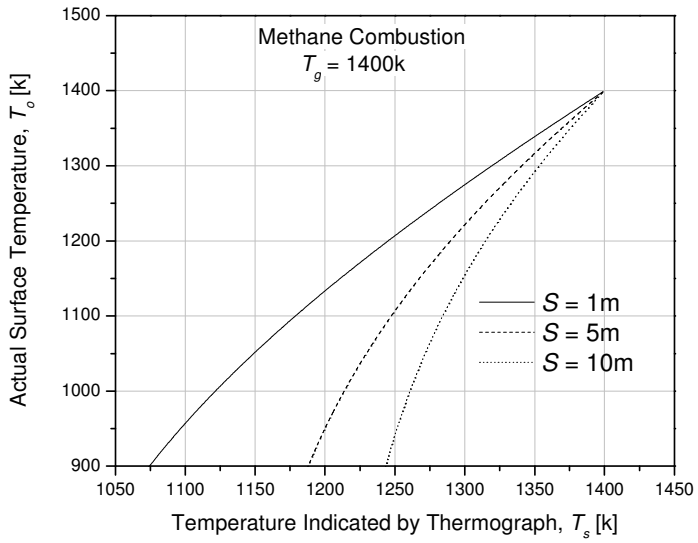

Figure 3. Variation of the actual temperature of the surface, T_0, with the temperature indicated in the thermograph, T_S, for three path lengths *S*.

In addition, the slope of the curve $T_0 \times T_S$ increases with the path length, making the temperature reading more prone to errors. This result shows that, in the thermograph measurement, it is important to choose the shortest distance between the surface and the thermograph for an accurate reading of the temperature.

Figure 4 shows in more detail the effect of the path length S on the temperature that is indicated in the thermograph. It is considered a medium temperature of 1400 K, and three temperatures of the surfaces, 900 K, 1100 K and 1300 K. In all cases, the temperature indicated in the sensor approximates of the actual of the actual temperature when the distance is small ($S \to 0$). When the distance increases, the slope of the curve tends to zero, but it is interesting to notice that the temperature indicated in the sensor does not tend to the temperature of the medium when $S \to \infty$. This is due to the transparent windows that exist in the medium. In fact, for large S the temperature, equation (18) shows that the temperature indicated in the thermograph tends to a temperature that is a weighting average of the medium and of the surface temperatures. Thus, the two limits for the temperature indicated in the thermograph are:

$$T_S \to T_0 \qquad \text{for } S \to 0 \tag{21}$$

$$T_S \to \left(\sum_{l=1}^{L} C_l \left(T_0 \right) \right) T_g + \left(1 - \sum_{l=1}^{L} C_l \left(T_0 \right) \right) T_0 \qquad \text{for } S \to +\infty \tag{22}$$

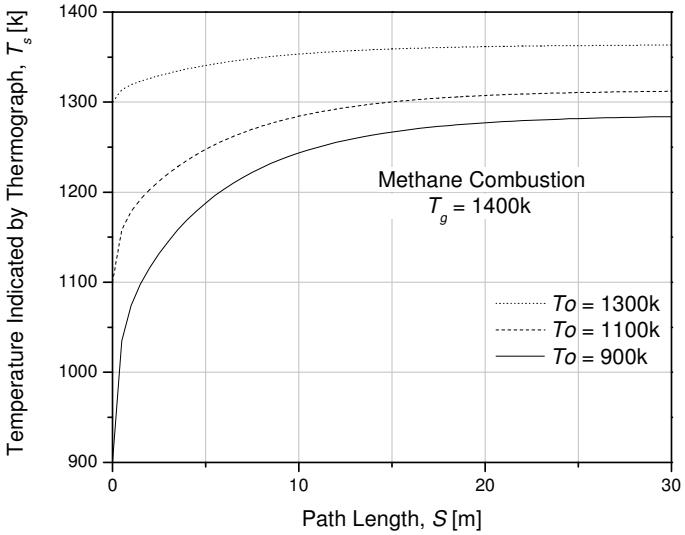

Figure 4. Variation of the temperature indicated in the thermograph, T_S, with the path length in the medium, S, for three different surface temperatures T_0.

4.1. Correlation for the Actual Temperature of the Surface

For practical use in the thermographic measurement of surface temperatures in systems having a medium formed by the stoichiometric combustion of methane, a correlation has been developed. The correlation was obtained by a multivariable non-linear regression analysis from the algorithm solution. The variables are the same that appear in equation (18), but the correlations intend to avoid the iterative procedure described in Section 3.2.3. The correlation is based on the following polynomial relations:

$$T_0 = \sum_{j=1}^{4} a_j T_S^{\,j-1} \tag{23}$$

$$a_j = \sum_{k=1}^{4} b_{j,k} S^{k-1} \tag{24}$$

$$b_{j,k} = \sum_{l=1}^{4} c_{j,k,l} T_g^{\,l-1} \tag{25}$$

The set of relations (23) to (25) provide a means to relate the temperature indicated in the thermograph, T_0, to the actual temperature of the surface, T_S, and to the medium temperature and path length. Following the procedure described in Section 3.2.3, a set of results were obtained for medium temperatures ranging from 1800 to 2400 K (with variation of 100 K), and for the following path lengths: 1, 2, 3, 4, 5, 10 and 15m. Therefore, the correlations are recommended to be used when the medium correspond to stoichiometric combustion of methane, and for gases temperatures are between 1800 and 2400 K, and path ranging from 0 to 15 m. A total of 29564 data points were obtained for the generation of the coefficients $c_{j,k,l}$, which are presented in Table 3.

Figures 5(a) and 5(b) illustrate a graphic comparison between the data generated from equation (8) and the data obtained from correlations (23) to (25) using the coefficients $c_{j,k,l}$ in Table 3. Two medium temperatures are considered T_g = 2000 K and 2200 K, for path lengths of 1 m, 5 m and 10 m. As seen in the figure, the correlations were capable of showing the behavior of the actual temperature as a function of the temperature indicated in the sensor. In most cases, the deviations between the data remained below 3%, but even for the worst cases the deviation did not exceed 5%.

Table 3. Coefficients $c_{j,k,l}$ for use in equation (25).

j	k	$c_{j,k,1}$	$c_{j,k,2}$	$c_{j,k,3}$	$c_{j,k,4}$
1	1	3.574 E+08	-5.548 E+05	2.743 E+01	-4.412 E-05
	2	-6.159 E+05	8.456 E+02	-3.896 E-01	5.952 E-05
	3	1.575 E+05	-2.325 E+02	1.109 E-01	-1.731 E-05
	4	-9.220 E+03	1.319 E+01	-6.162 E-03	9.494 E-07
2	1	-3.866 E+02	6.548 E-01	-3.400 E-04	5.651 E-08
	2	1.091 E+03	-1.485 E+00	6.798 E-04	-1.036 E-07
	3	-2.351 E+02	3.546 E-01	-1.719 E-04	2.721 E-08
	4	1.512 E+01	-2.184 E-02	1.030 E-05	-1.599 E-09
3	1	6.811 E-02	-1.721 E-04	1.054 E-07	-1.921 E-11
	2	-6.630 E-01	8.926 E-04	-4.052 E-07	6.145 E-11
	3	1.108 E-01	-1.719 E-04	8.513 E-08	-1.369 E-11
	4	-8.090 E-03	1.181 E-05	-5.618 E-09	8.789 E-13
4	1	2.232 E-05	-1.382 E-08	4.754 E-13	6.338 E-16
	2	1.384 E-04	-1.846 E-07	8.304 E-11	-1.251 E-14
	3	-1.616 E-05	2.616 E-08	-1.333 E-11	2.189 E-15
	4	1.412 E-06	-2.083 E-09	1.001 E-12	-1.578 E-16

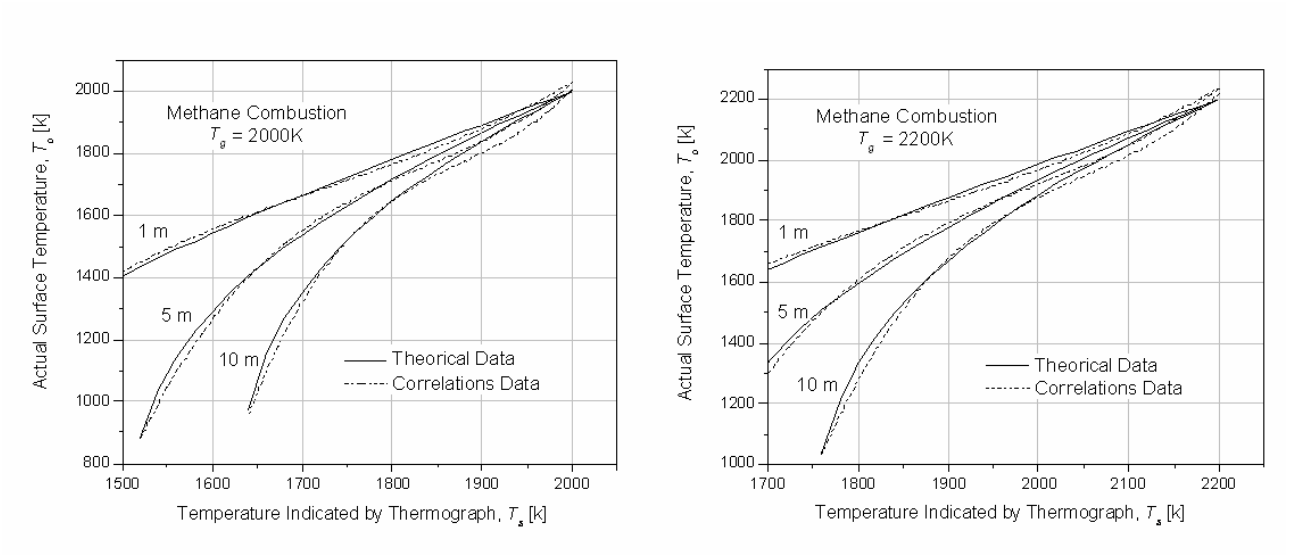

Figure 5. Variation of the actual temperature of the surface, T_0, with the temperature indicated in the sensor, T_S: comparison of the theorical results from equation (18) with the results from correlations (23) to (25).

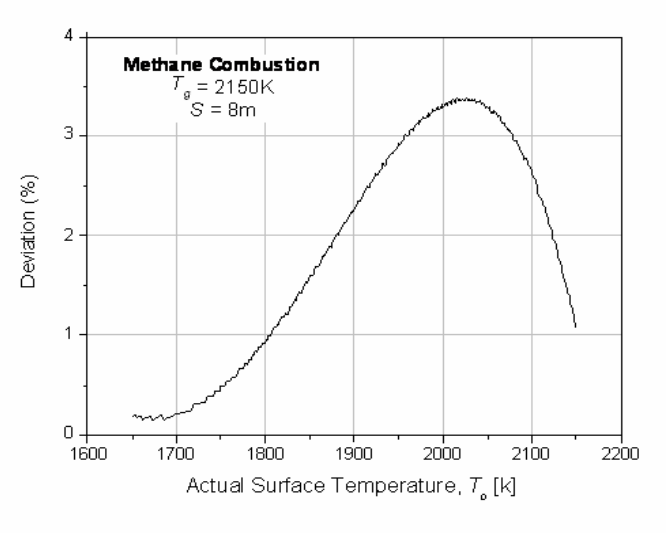

Figure 6. Deviation using the correlations data.

Another evaluation of the proposed correlation is shown in Fig. 6, which presents the deviation of the correlation for different values of the actual temperature of the surface. For this case, it was considered a path length of S = 8 m and a medium temperature of T_g = 2150 K, that is, two conditions that were not considered for the generation of the correlating points. This is therefore an interesting case for evaluation of the correlation. As seen in Fig. 6, the relative error remained less than 3% for most part of the plot. This behavior was observed for several other tests of the correlation, indicating that it can be used with a confidence that is above 95%.

6. CONCLUSIONS

This paper presented a methodology to correct the temperature indicated by thermograph for remote measurement of surfaces temperature. This correction is necessary when there is a participating medium between the surface and the thermograph sensor, as with measurements of internal surfaces of gas turbines, furnaces and other combustion systems. The correction of the temperature was based on the solution of the radiative transfer equation for participating media, considering absorption and emission, but not scattering. The methodology was applied to a gaseous mixture with a molar concentration of 10% of water vapor, 10% of carbon dioxide, the remaining species being a non-participating medium, such as air or nitrogen. Such a mixture is typical of the stoichiometric combustion of methane in air. Due to the non-linear nature of the problem, the solution involved an iterative algorithm.

The examples shown in this paper revealed that the temperature indicated by the thermograph sensor can be considerably different from the actual temperature of the surface, especially when there is a large difference between the temperatures of the surface and of the medium, and also for large path lengths in the medium. One interesting result is that for very large paths in the medium, the temperature indicated by the thermograph will be a weighted average of the temperatures of the medium and of the surface, where the weighting coefficients correspond to the fraction of the blackbody energy, at the medium temperature, in the participating and in the transparent windows of the spectrum.

For fast application in engineering, a correlation was formulated to relate the actual temperature of the surface to the temperature indicated by the thermograph sensor, the medium temperature and the path length in the medium. The correlation involved polynomial relations, and presented a deviation with the original data of less than 3% for most cases, with maximum deviation below 5%. Although the correlation was developed for a specific gas mixture, the methodology can be readily applied for generation of correlations for other participating media.

7. ACKNOWLEDGEMENTS

The second author thanks CNPq for the support under a Doctor Degree scholarship. The third author thanks CNPq for research grant 304535/2007-9.

8. REFERENCES

Denison, M. K.; Webb, B.W., 1995, “The Spectral Line-Based Weighted-Sum-of-Gray-Gases Model for H20/CO2 Mixtures”**,** J Heat transfer, 117:788-92.

Galarça, M. M.; Maurente, A.; Vielmo, H. A.; França, F. H. R., 2008, "Correlations for the Weighted-Sum-of-Gray-Gases Model Using Data Generated from the Absorption-Line Blackbody Distribution Function", 12ht Brazilian Congress of Thermal Engineering and Sciences.

Holman, J. P., "Experimental Methods for Engineers", 6.ed. New York: Mcgraw-Hill.

Hottel, H. C.; Sarofim, A. F., 1967, "Radiative Transfer", New York: Mcgraw-Hill Book Company.

Incropera, F. P.; Dewitt, D. P. "Fundamentos de Transferência de Calor e de Massa", 2002, 5.ed. Rio de Janeiro, LTC Editora.

Maurente, A.; Vielmo, H. A.; França, F. H. R., 2007, "A Monte Carlo Implementation to Solve Heat Transfer in Non-Uniform Media with Spectrally Dependent Properties", J Quantitative Spectroscopy and Radiative Transfer, 108:295-307.

Maurente, A.; Vielmo, H. A.; França, F. H. R., 2008, "Comparison of the Standard Weighted-Sum-of-Gray-Gases with the Absorption-Line Blackbody Distribution Function for the Combustion of Radiative Heat Transfer in H2O/CO2 Mixtures", J Quantitative Spectroscopy and Radiative Transfer, 109:1758-1770.

Siegel, R.; Howell, J.R., 2002, "Thermal Radiation Heat Transfer", 4.ed. New York: Taylor & Francis.

Smith, T. F.; Shen, Z. F.; Friedman, J. N., 1985, "Evaluation of Coefficient for the Weighted-Sum-of-Gray-Gases Model", J Heat Transfer, 104:602-8.

Taylor, P. B.; Foster, P. J., 1974, "The Total Emissivities of Luminous and Non-Luminous Flames", J Heat Mass Transfer, 17:1591-605.

8. Copyright notice